INORGANIC CHEMISTRY
FRONTIERS

RESEARCH ARTICLE

View Article Online
View Journal | View Issue

Cite this: *Inorg. Chem. Front.*, 2025, **12**, 4645

Barium(II)-based molecular perovskite energetic compounds for next-generation pyrotechnic materials†

Chen-Xi Yu, Le Ye, Hao Zhuo, Yun-Fan Yan and Wei-Xiong Zhang *

Traditional pyrotechnic compositions formed by mechanically mixing flammable and oxidative agents face the problems of complex formulations, inaccurate chemical stoichiometry, and inefficient colour-producing reactions. Emerging molecular perovskite energetic materials with embedded ternary ions have evolved into a new platform for developing explosives, propellants, ignition materials, and energetic biocides, taking advantage of their easy preparation and high adjustability. However, their potential in pyrotechnic applications has not yet been investigated. Herein, by assembling barium(II) perchlorate with imidazolium (Him^+) and quinuclidinium (Hqe^+) ions, we obtained two new energetic compounds, $(Him)(Ba)(ClO_4)_3$ (IBP) with a cubic perovskite structure, and $(Hqe)_2(Ba)(ClO_4)_4$ (QBP) with a layered perovskite structure. Both IBP and QBP have decomposition peak temperatures exceeding 290 °C and much higher moisture stabilities than barium perchlorate. With a layered structure, QBP has significantly lower friction sensitivity (144 N) than IBP (5 N). Moreover, the tight stacking of barium(II), oxidative perchlorate ions, and carbon-rich fuel components at the molecular level allows QBP to exhibit high-efficiency and stable combustion, outputting a maximum combustion pressure of up to 550 kPa, a maximum pressure pulse rate of up to 10.48 MPa s^{-1}, and a bright green flame. These findings demonstrate well that molecular perovskite energetic compounds integrating a luminescent component, oxidative anions, and organic cations are promising contenders for next-generation pyrotechnic materials.

Received 14th February 2025,
Accepted 2nd April 2025

DOI: 10.1039/d5qi00442j

rsc.li/frontiers-inorganic

1. Introduction

Pyrotechnic compositions are intricately designed to control and leverage a spectrum of effects such as illumination, sound generation, chromatic display, gas release, and smoke production upon ignition.[1] These compositions serve diverse purposes spanning the civilian, military, and aerospace sectors. Notably, firework exhibitions are pivotal features in national or religious festivities and commemorations, including grand events like the Paris Olympics, captivating many people.[2] Typically, fireworks consist of a blend of oxidizers, fuels, and binders, producing coloured flames primarily through the combustion of alkali and alkaline-earth metal salts.[3] Barium salts together with chlorinated organic materials are adopted to provide green flames in traditional pyrotechnic compositions, by producing the metastable green-light-emitting species barium(I) monochloride (BaCl) or barium(I) monohydroxide (BaOH) with a higher colour purity than the boron-based formulations.[1,4,5] However, these classic formulations, characterized by high moisture absorption and non-energetic chlorinated binders, face challenges in assessing the uniformity of powder blending, resulting in an unreliable green flame.

To counteract the issues of low combustion heat, inaccurate chemical stoichiometry and difficulties in preparation, a new wave of highly energetic pyrotechnic materials has emerged, encompassing nitrogen-rich compositions and energetic metal coordination compounds.[6–20] For example, 4-chloro-3,5-dinitropyrazolidebarium salts, leading to striking green flames and excellent combustion performance, benefit from high-energy polynitrogen organic molecules.[6] However, challenges persist in achieving assembly efficiency and performance adjustability. There is an urgent need to seek next-generation pyrotechnic materials with high combustion heat, reliable ignition, colour purity, and simple synthesis processes.

Molecular perovskite energetic materials proposed by our team in 2018, as a type of emerging non-traditional energetic material relying on the self-assembly of multiple ions rather than covalent modification of organic molecules, have attracted widespread attention due to their advantages such as

MOE Key Laboratory of Bioinorganic and Synthetic Chemistry, School of Chemistry, IGCME, Sun Yat-Sen University, Guangzhou 510275, China.
E-mail: zhangwx6@mail.sysu.edu.cn

†Electronic supplementary information (ESI) available. CCDC 2400712 and 2400713. For ESI and crystallographic data in CIF or other electronic format see DOI: https://doi.org/10.1039/d5qi00442j

a wide range of raw material sources, simple preparation, high stability, and easy adjustability.[21] These single-phase crystalline materials are formed by the alternating close arrangement of A-site organic cations, B-site inorganic cations and X-site oxidative anions in the perovskite crystal structures.[22–24] In the past few years, the endeavours in designing new molecular perovskite energetic crystals have created a diverse array of varieties in cubic or hexagonal ABX_3-type perovskite structures (Fig. 1) for specified energetic applications, such as ignition materials, propellants, biocidal agents, primary explosives, and secondary explosives.[25–28] Regarding inorganic barium salts such as $Ba(ClO_3)_2$ and $Ba(ClO_4)_2$ (BP), which are adopted in classic green coloured formulations, barium-based molecular perovskite energetic compounds, as organic–inorganic hybrid compounds mimicking classic formulations at the molecular level, are expected to effectively yield green-light-emitting BaCl or BaOH species, and hence to be promising pyrotechnic materials combining striking green flames, excellent combustion performance, and simple synthesis processes. However, reports on barium-based molecular perovskites are still relatively scarce, and none of them consider potential energetic properties.[29,30]

To this end, we employed ClO_4^- as X-bridges, Ba^{2+} as the B-site cation, and diverse organic A-site cations to construct barium-based molecular perovskite energetic compounds. Our efforts have successfully yielded two new compounds, (Him)$(Ba)(ClO_4)_3$ (IBP, Him^+ = imidazolium) and $(Hqe)_2(Ba)(ClO_4)_4$ (QBP, Hqe^+ = quinuclidinium), which possess a cubic perovskite structure and a layered perovskite structure, respectively. By combining single-crystal structural analysis, thermal analysis, *etc.*, we comprehensively studied their structures, thermal stabilities, and combustion performance. We found that both IBP and QBP have high decomposition peak temperatures exceeding 290 °C and much better moisture stabilities than BP. In particular, the layered structure endows QBP with a significantly lower friction sensitivity (144 N) than IBP (5 N). Moreover, combustion tests showed that the tight stacking of barium(II), oxidative perchlorate ions, and carbon-rich fuel components at the molecular level allows QBP to exhibit high-efficiency and stable combustion, outputting a combustion pressure of up to 550 kPa, a maximum pressure pulse rate of up to 10.48 MPa s^{-1}, and a bright green flame. A possible mechanism is proposed to explain why the combustion of QBP could emit such a bright green flame.

2. Experimental

Caution! Although they were safe in the course of this research, these energetic materials need to be handled with extreme care.

2.1. General methods

All chemicals were obtained from commercial sources and used without further purification. Decomposition temperatures were measured *via* DTA with an OZM Research DTA

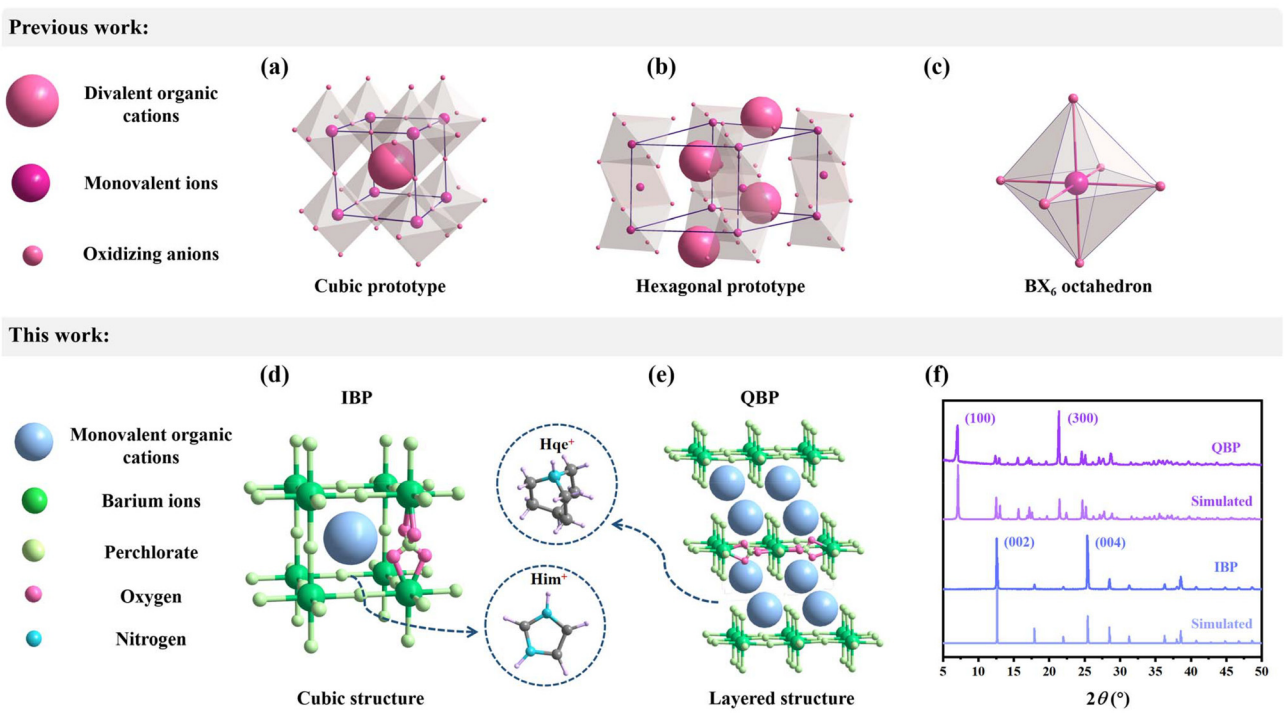

Fig. 1 The two typical energetic perovskite structures (a and b) based on different linkages of BX_6 octahedra (c). The three-dimensional molecular packing of IBP (d) and the two-dimensional molecular packing of QBP (e). The PXRD patterns (f) of IBP and QBP. For clarity, some oxygen atoms are omitted.

552-Ex instrument at a rate of 10 °C min^{-1} and in a range from RT to 400 °C under air. The PXRD patterns (Cu Kα) for identifying the phase purity were collected by Bragg–Brentano geometry on a Bruker Avance D8 diffractometer. Detonation parameters were calculated using DFT calculation and the extended K–J equation. Friction sensitivity was tested on an FSKM 10 BAM friction apparatus.

2.2. Synthetic procedures

Synthesis of $(Him)(Ba)(ClO_4)_3$ (IBP). 670 mg of barium perchlorate (2 mmol) and 70% perchloric acid solution (2 mL) were added to H_2O (10 mL); then 140 mg of imidazole (2 mmol) was added into the above solution slowly. A white solid was collected by filtration and washed three times with ethanol.

Synthesis of $(Hqe)_2(Ba)(ClO_4)_4$ (QBP). 670 mg of barium perchlorate (2 mmol) and 70% perchloric acid solution (2 mL) were added to H_2O (10 mL); then 450 mg of quinuclidine (4 mmol) was added into the above solution slowly. A white solid was collected by filtration and washed three times with ethanol.

3. Results and discussion

3.1. Structure analysis

Single-crystal X-ray diffraction at 298 K shows that IBP has a cubic perovskite structure, while QBP has a layered perovskite structure. In detail, IBP crystallizes in the cubic space group $Fm\bar{3}c$ (Table 1). Each Ba^{2+} ion engages with 12 oxygen atoms from six surrounding ClO_4^- anions, while each ClO_4^- anion connects two neighbouring Ba^{2+} ions, creating a three-dimensional anionic coordination lattice to host the fuel cations, *i.e.*, Him^+ cations. Remarkably, the Him^+ cation shows a 24-fold crystallographically disordered state at 298 K, implying highly rotational dynamics of a relatively small cation in relatively large cage-like confined spaces. Interestingly, the larger size of Hqe^+ compared to Him^+ facilitates the formation of a layered perovskite structure in QBP. In detail, QBP crystallizes in the monoclinic space group $P2_1/c$ at 298 K (Table 1). Each Ba^{2+} ion coordinates with 12 oxygen atoms from six neighbouring ClO_4^- anions, among which only four equatorial ClO_4^- anions act as bridging ligands, while the axial ones act as terminal ligands, to form two-dimensional $\{Ba(ClO_4)_4\}_n^{2n-}$ coordination layers. The Hqe^+ cations are distributed between the layers, and their –NH groups form hydrogen bonds interacting with the oxygen atoms of the terminal ClO_4^- anions, further stabilizing the entire crystal structure. In summary, by assembling into perovskite structures, the non-energetic organic fuel cations, halogen-containing oxidative anions, and luminescent metal ions can be efficiently integrated at the molecular level. The powder X-ray diffraction (PXRD) patterns for IBP and QBP are presented in Fig. 1f. The powder phase purity was confirmed by the close matches of the experimental PXRD patterns with the corresponding simulated ones from the single-crystal structures.

Table 1 Crystallographic data and structural refinements for IBP and QBP

Compound	IBP	QBP
Formula	$C_3H_5BaCl_3N_2O_{12}$	$C_{14}H_{28}BaCl_4N_2O_{16}$
Formula weight	504.78	759.52
Temperature/K	298(2)	298(2)
Crystal system	cubic	monoclinic
Space group	$Fm\bar{3}c$	$P2_1/c$
a/Å	14.0014(9)	12.970(2)
b/Å	14.0014(9)	10.3066(8)
c/Å	14.0014(9)	10.146(1)
V/Å^3	2744.8(5)	1298.7(2)
β/°	90	106.744(5)
Z	8	2
D_c/(g cm^{-3})	2.443	1.942
R_1 $[I > 2\sigma(I)]^a$	0.0197	0.0396
wR_2 $[I > 2\sigma(I)]^b$	0.0433	0.1176
R_1 (all data)	0.0233	0.0510
wR_2 (all data)	0.0451	0.1243
GOF	1.137	1.128
CCDC	2400712	2400713

$^a R_1 = \sum||F_o| - |F_c||/\sum|F_o|$. $^b wR_2 = [\sum w(F_o^2 - F_c^2)^2/\sum w(F_o^2)^2]^{1/2}$.

3.2. Thermal stability

The thermal stabilities of IBP and QBP were examined using differential thermal analysis (DTA) measurements at heating rates of 5 °C min^{-1} and 10 °C min^{-1} in air. As shown in Fig. 2, at a heating rate of 5 °C min^{-1}, IBP and QBP exhibit clear and sharp exothermic peaks at 357 °C and 298 °C, respectively, indicating rapid structural collapse and decomposition. At a heating rate of 10 °C min^{-1}, the thermal decomposition peaks of QBP and IBP slightly shifted to higher temperatures, *i.e.*, 360 °C and 300 °C, respectively. These observations indicate that both IBP and QBP have much higher thermal stabilities than cyclotrimethylenetrinitramine (RDX, 210 °C), one of the widely used military explosives. Their higher thermal stabilities than most organic explosives could be attributed to strong intra-ionic covalent bonds and attractive inter-ionic Coulomb interactions, as well as hydrogen bonds. The moderately decreased decomposition temperatures compared with inorganic BP (melting point, 505 °C) indicate that the integrated organic cations promote the decomposition reaction to achieve reliable ignition and rapid decomposition.

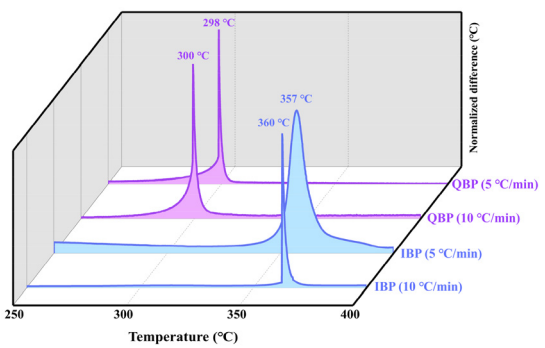

Fig. 2 DTA curves of IBP and QBP at heating rates of 5 and 10 °C min^{-1} in air.

3.3. Hygroscopicity experiments

As severe hygroscopicity usually occurs in perchlorate salts, the hygroscopic properties of IBP, QBP, and BP were explored under ambient conditions at 100% and 86% relative humidity (RH), as shown in Fig. 3. The results clearly indicated that both IBP and QBP have notably higher moisture stability than BP. In detail, after remaining at 86% RH for 1000 h, IBP and QBP showed weight increases of 0.01% and 4.23%, respectively, while BP showed a much higher weight increase of 11.73%. Even after remaining for the same duration at 100% RH, BP increased in weight by 13.18%, while IBP and QBP showed lower weight increases of 4.51% and 8.82%, respectively. The integrated organic cations endow IBP and QBP with lower hygroscopicity than BP. Such an improvement in hygroscopicity for ternary-ionic salts compared with binary-ionic salts has also been observed in other molecular perovskite energetic compounds.[25]

The moisture absorption order (IBP < QBP < BP) is associated with the different strengths of the perchlorate-involved coordination bonds and intermolecular interactions. Specifically, all oxygen atoms of the perchlorate anions in IBP and QBP are coordinating with the adjacent Ba(II) ions, whereas only some oxygen atoms coordinate with Ba(II) ions in BP. In addition, as listed in Table S1 (see ESI†), the average Ba–O bond lengths in IBP and QBP are 2.898 Å and 2.906 Å, respectively, and both are shorter than that in BP (3.062 Å). The stronger perchlorate-involved coordination bonds help to reduce the affinity of perchlorate for water, resulting in a lower hygroscopicity for IBP and QBP. Regarding the hygroscopicity difference between IBP and QBP, the smaller-sized Him^+ cation can induce Ba^{2+} and ClO_4^- to form a stable cubic coordination structure, reducing the probability of binding with water molecules for ClO_4^- ions in IBP, whereas the terminal ClO_4^- ions in the coordination layers and the weaker inter-layer interactions allow the external water molecules to penetrate the interior, endowing QBP with a higher hygroscopicity than IBP.

3.4. Sensitivity and stress–strain curve simulation

The impact sensitivity measured by using a BFH 10 BAM apparatus is 23 J for IBP and 25 J for QBP, similar to those of most known molecular perovskite energetic compounds such as DAP-4 (23 J).[21] Such an impact insensitivity could be ascribed to the similar dense perovskite crystal structures together with the buffering effects of inter-ionic interactions between the stable ions. The friction sensitivity was measured by FSKM 10 BAM, disclosing a large difference in friction sensitivity between IBP (5 N) and QBP (144 N). The friction sensitivity of IBP, possessing a three-dimensional coordination structure, is comparable to known analogous energetic compounds with cubic perovskite structures.[21] In contrast, upon employing a relatively spherical A-site cation (*i.e.*, Hqe^+) to provide layered structural characteristics, the resulting QBP has a much-decreased friction sensitivity.

To further explore the underlying mechanism, we utilized the CASTEP program to calculate the stress–strain curves for IBP and QBP (Fig. 4). Characterization using PXRD (Fig. 1f) indicates that the preferred crystallographic orientations for QBP are (100) and (300) planes, while they are (002) and (004) planes for IBP. Therefore, simulations were conducted on crystal planes perpendicular to these preferred orientations. It is observed that the stress increases with strain, highlighting the significant dependence of IBP and QBP on strain variations. IBP exhibits higher steady-state stresses when the strain increases from 6% to 9%, indicating that its relatively "hard" cubic structure cannot provide sufficient buffering to counter friction stimulation, resulting in higher friction sensitivity. In contrast, QBP maintains lower steady-state stresses as the strain increases from 2% to 9%, due to its "easy sliding" layered structure, which suppresses hotspot accumulation and achieves friction insensitivity.

3.5. Detonation parameters

The detonation parameters of IBP and QBP were estimated by using density functional theory (DFT) and the extended Kamlet–Jacobs (K–J) equations, and the results are listed in

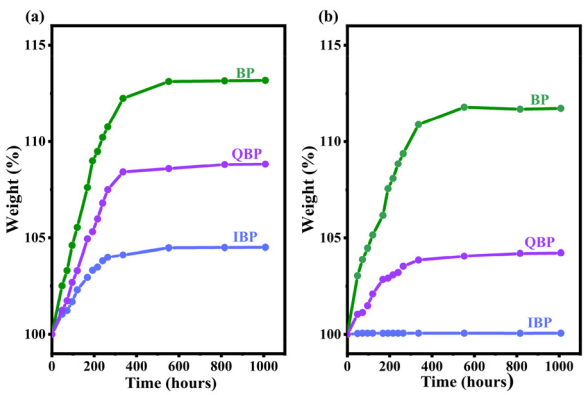

Fig. 3 Hygroscopic curves of BP, QBP, and IBP at room temperature at 100% RH (a) and 86% RH (b) for 1000 h.

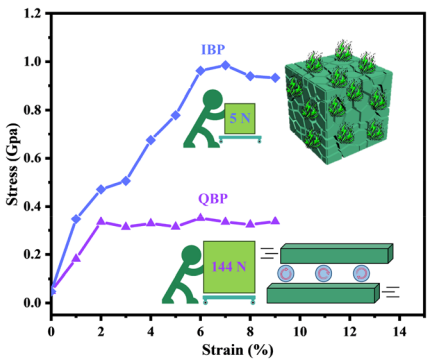

Fig. 4 Stress–strain curves and illustration of the frictional force for IBP and QBP.

Table 2 Comparison of the detonation performance of IBP, QBP, TNT and black powder

Compound	ρ/g cm^{-3}	D/km s^{-1}	P/GPa	Q/kJ g^{-1}	OB[a]/%	FS/N	IS/J
TNT[31]	1.65	6.90	20.0	4.36	−74	360	15
IBP	2.44	6.26	20.5	2.20	12.7	5	23
QBP	1.94	7.64	16.9	2.78	−52.7	144	25
Black powder[28]	—	<0.5	—	2.76	—	Sensitive	Sensitive

ρ: crystal density; D: detonation velocity; P: detonation pressure; Q: detonation heat; FS: friction sensitivity; IS: impact sensitivity. [a] Oxygen balance based on CO_2 for $C_aH_bN_cM_dCl_eO_f$, with M as a metal ion. OB = $1600[f - 2a - (b - e + 2d)/2]/M_W$, where M_W is the molecular weight.

Table 2. Compared to QBP's layered structure with a crystal density of 1.94 g cm^{-3}, IBP's cubic structure leads to a higher crystal density (2.44 g cm^{-3}) and apparent calculated detonation pressure (20.5 GPa). The positive oxygen balance of IBP reaching 12.7% results in an excess of oxygen that cannot be converted to carbon dioxide, giving a detonation heat (2.20 kJ g^{-1}) lower than TNT (4.36 kJ g^{-1}) and black powder (2.76 kJ g^{-1}). In contrast, the carbon-rich QBP, with a much negative oxygen balance (−52.7%), cannot convert all carbon into carbon dioxide either, leading to a detonation heat (2.78 kJ g^{-1}) slightly higher than IBP but close to black powder. Such a moderate detonation heat is beneficial for maintaining stable combustion, enabling QBP to be a promising pyrotechnic material.

3.6. Combustion experiments for QBP

Excessive oxygen in IBP may lead to the formation of barium oxide as a byproduct, adversely affecting the emission of a green flame. In this sense, QBP with a negative oxygen balance and lower friction sensitivity has more promising potential for pyrotechnic application. Therefore, QBP was submitted to investigate the combustion performance. First, the combustion experiments were conducted for QBP by employing a 50 mL constant-volume combustion cell, in accordance with the GJB 770B-2005 standard (Fig. S1†). For a better comparison, tests were also conducted on BP, (Hqe)(ClO_4) (QP), and their binder-free mixture (named QP/BP, consisting of QP and BP in a 2 : 1 molar ratio), under the same conditions. As shown in Fig. 5a and b, the decomposition of BP outputs negligible

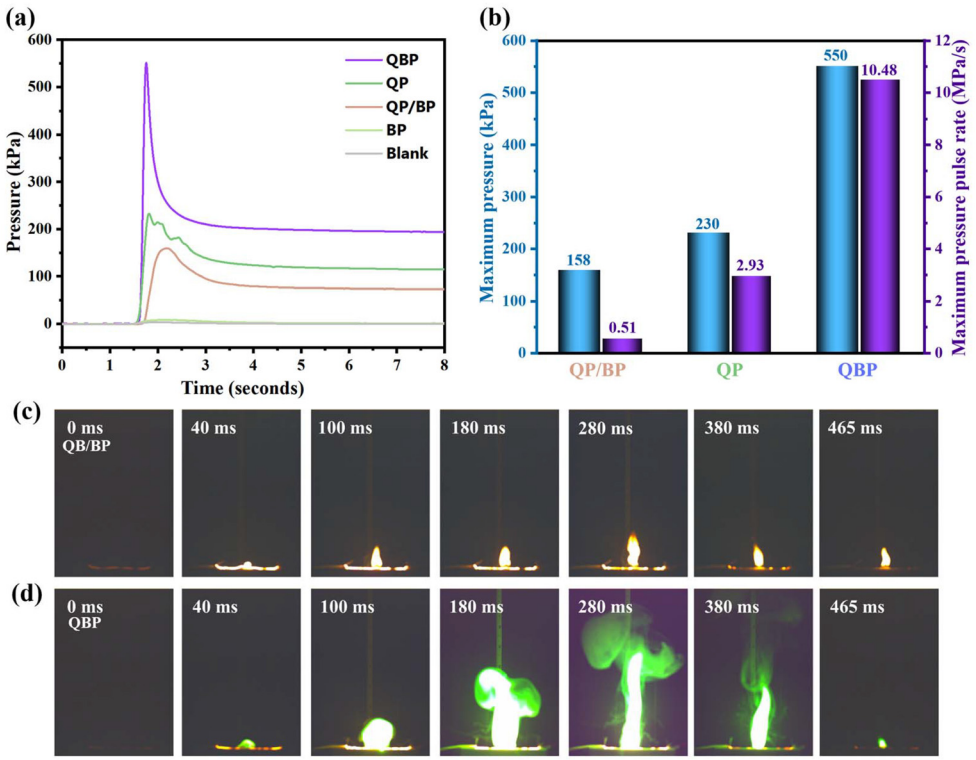

Fig. 5 Combustion pressure curves (a), peak pressures and maximum pressure pulse rates (b) of QBP, QP and the QP/BP mixture (molar ratio: 2 : 1). High-speed photography of combustion for the QP/BP mixture (c) and QBP (d).

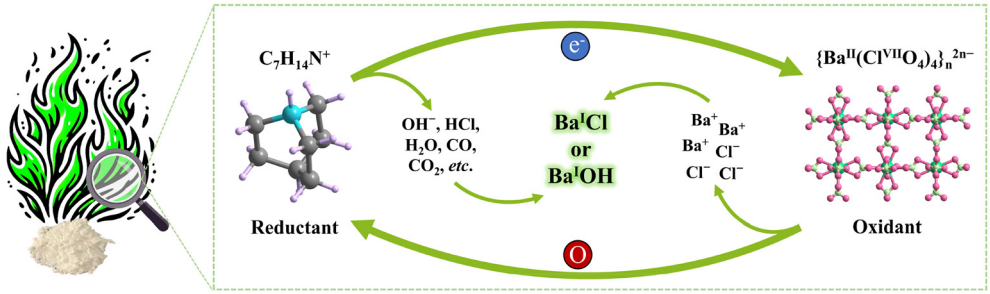

Fig. 6 A possible combustion mechanism of QBP to emit a bright green flame.

pressure, and the maximum combustion pressures achieved by QP and QP/BP were 230 kPa and 158 kPa, respectively, and both are significantly lower than that achieved by QBP (550 kPa). Similarly, the maximum pressure pulse rate of QBP reaches 10.48 MPa s^{-1}, far exceeding those of QP (2.93 MPa s^{-1}) and QP/BP (0.51 MPa s^{-1}).

To further investigate the combustion flame for QBP, high-speed photography with a frame rate of 1000 frames per second was employed to record the combustion for the QP/BP mixture and QBP under same conditions (using 60 mg samples). As shown in Fig. 5c and d, high-speed photography clearly revealed significant differences in ignition behaviours between the QP/BP mixture and QBP. Specifically, the ignition process of the QP/BP mixture was relatively difficult, whereas QBP could be easily ignited under same test conditions. Taking the photo shots at the 280 ms as examples, the QP/BP mixture only emitted a faint yellow glow, indicating that the BP component had not been effectively ignited, whereas QBP emitted a very bright green flame with a much higher flame height.

3.7. A possible combustion mechanism

The flame emission wavelength is an important factor for the investigation of pyrotechnics, and the flame emission spectrum of QBP was measured using a visible spectrometer. Spectral analysis (Fig. S2†) revealed dominant emissions in the green spectral region (475–540 nm), with intense emission peaks at 513 nm and 524 nm. The colour purity of 82% meets the US Army's requirement.[1] The observed emission in the green spectral region matches well with the emission spectra of BaCl or BaOH species, where photons are emitted as electrons transition from higher-energy excited states to lower-energy states in the wavelength range of 500–540 nm.[32] These findings demonstrate well the advantage of a ternary-ionic assembly in a perovskite structure in providing high-efficiency and stable combustion that endows QBP with lower ignition energy requirements, faster reaction kinetics, and a brighter green flame. As illustrated in Fig. 6, a possible mechanism for producing the bright green flame was proposed. The carbon-rich organic cation Hqe^+ provides a reducing effect that converts Ba(II) to Ba(I) and Cl(VII) to Cl^-, while simultaneously producing hydrogen-containing species such as OH^- and HCl. This process generates a large number of metastable species (*e.g.*, BaCl or BaOH) that emit green flames through radiative transitions. The carbon-rich Hqe^+ could inhibit the formation of luminescent inactive barium oxide during combustion, providing an additional contribution to the colour purity of the flame. Moreover, the presence of excess carbon and hydrogen over oxygen, namely, the negative oxygen balance of −52.7%, further prevents the detonation, but sustains combustion, thereby prolonging the lifespan of the metastable BaCl or BaOH.

4. Conclusions

By introducing barium(II) ions as B-site ions and utilizing a molecular self-assembly strategy, two barium-based energetic perovskite compounds, IBP and QBP, have been successfully synthesized. The single-crystal structural analyses showed that the sizes and shapes of the A-site organic cations have a strong influence on their crystal structures. The smaller and highly-disordered Him^+ organic cations endow IBP with a cubic perovskite structure, while the larger Hqe^+ organic cations endow QBP with a layered perovskite structure. Being organic–inorganic hybrid compounds, both IBP and QBP have high thermostabilities with decomposition peak temperatures exceeding 290 °C and much higher moisture stabilities than inorganic barium perchlorate. It is intriguing that the transition between cubic and layered perovskite structures can bring about an improvement in the friction stability from 5 N to 144 N. The dense stacking of oxidative anions and organic cations in QBP leads to high-efficiency combustion with a high combustion pressure (550 kPa) and a maximum pressure pulse rate of up to 10.48 MPa s^{-1}, much exceeding those of the mixture of its raw materials. Moreover, the carbon-rich organic cations endow QBP with a negative oxygen balance to give a suitable combustion heat that not only results in reliable ignition but also contributes to the generation of metastable species BaCl or BaOH for emitting a bright green flame. As demonstrated by QBP, the present molecular perovskite energetic compounds integrating a luminescent component, oxidative anions, and organic cations provide many new opportunities for the development of pyrotechnic materials. Such ternary-ionic integrated materials may unlock a novel luminescence

mechanism for flame colouration, indicating the arrival of next-generation pyrotechnic materials.

Author contributions

Wei-Xiong Zhang designed the research. Chen-Xi Yu conducted the synthetic experiments and most measurements. Le Ye provided assistance in the single-crystal XRD analysis. Hao Zhuo provided assistance in the CASTEP program. Yun-Fan Yan provided assistance in the combustion tests.

Data availability

The data supporting this article have been included as part of the ESI.†

Conflicts of interest

There are no conflicts to declare.

Acknowledgements

This work was supported by NSFC (U2341287 and 22488101), Guangzhou Science and Technology Programme (2024A04J6499), Fundamental Research Funds for the Central Universities, Sun Yat-Sen University (23lgzy001).

References

1 S. Kanitkar, D. Haynes, E. M. Sabolsky and B. Chorpening, A review of coloured light production by pyrotechnic materials, *Propellants, Explos., Pyrotech.*, 2023, **48**, e202300012.
2 J. Gluck, T. M. Klapötke, M. Rusan, J. J. Sabatini and J. Stierstorfer, A strontium- and chlorine-Free pyrotechnic illuminant of high colour purity, *Angew. Chem., Int. Ed.*, 2017, **56**, 16507–16509.
3 W.-S. Dong, X. Wang, C. Zhang, L. Zhang, Y. Hu, W. Cao, X. Wu, T. Wang and J.-G. Zhang, Multidimensional energetic coordination polymers as flame colourants: intriguing architecture and excellent performance, *Cryst. Growth Des.*, 2022, **22**, 5449–5458.
4 A. Ambekar, M. Kim and J. J. Yoh, Characterization of display pyrotechnic propellants: coloured light, *Appl. Therm. Eng.*, 2017, **110**, 1066–1074.
5 J. J. Sabatini, J. C. Poret and R. N. Broad, Boron carbide as a barium-free green light emitter and burn-rate modifier in pyrotechnics, *Angew. Chem., Int. Ed.*, 2011, **50**, 4624–4626.
6 W.-S. Dong, H. Zhang, Q. Tariq, Z. Li, C. Zhang, X. Wu, Q. Yu, Z. Li, Z. N. Zhou and J.-G. Zhang, Metal salts of 4-chloro-3,5-dinitropyrazole for promising ecoFriendly primary colours pyrotechnics, *Inorg. Chem.*, 2023, **62**, 14559–14567.
7 W. Cao, T. Wang, H. Mei, W. Dong, Q. Tariq, L. Yin, Z. Li and J.-G. Zhang, Access to green pyrotechnic compositions via constructing coordination polymers: a new approach to the application of 3,4-dinitropyrazole, *ACS Appl. Mater. Interfaces*, 2022, **14**, 32084–32095.
8 Y.-F. Yan, J.-G. Xu, F. Wen, Y. Zhang, H.-Y. Bian, B.-Y. Li, N.-N. Zhang, F.-K. Zheng and G.-C. Guo, Sensitive structural motifs separately distributed in azide-based 3D EMOFs: a primary explosive with an excellent initiation ability and enhanced stability, *Inorg. Chem. Front.*, 2022, **9**, 5884–5892.
9 A. M. W. Dufter, T. M. Klapötke, M. Rusan and J. Stierstorfer, Comparison of functionalized lithium dihydrobis(azolyl) borates with their corresponding azolates as environmentally friendly red pyrotechnic colouring agents, *ChemPlusChem*, 2020, **85**, 2044–2050.
10 T.-W. Wang, C. Zhang, M.-Q. Xu, B.-L. Kuang, Z.-M. Xie, Z.-J. Lu, Z.-X. Yi, Y. Li and J.-G. Zhang, The combined effect of pyrazole and amino groups: preparation of novel energetic coordination compounds with high ClO_4^- content, *Inorg. Chem. Front.*, 2023, **10**, 5311–5319.
11 T. Wang, J. Zhou, Q. Zhang, L. Zhang, S. Zhu and Y. Li, Novel 3D cesium(I)-based EMOFs of nitrogen-rich triazole derivatives as "green" orange-light pyrotechnics, *New J. Chem.*, 2020, **44**, 1278–1284.
12 X. Chen, S. Wang, Y. Chen, Y. Hu, C. Zhang, Z. Guo and H. Ma, Alkaline earth metal salts of 3,6-bis-nitroguanyl1,2,4,5-tetrazine: promising perchlorate-free environmentally friendly pyrotechnic components, *Appl. Organomet. Chem.*, 2021, **36**, e6497.
13 K.-C. Wang, T.-L. Liu, Y.-H. Jin, S. Huang, N. Petrutik, D. ShemTov, Q.-L. Yan, M. Gozin and Q.-H. Zhang, "Tandem-action" ferrocenyl iodocuprates promoting low temperature hypergolic ignitions of "green" EIL–H_2O_2 bipropellants, *J. Mater. Chem. A*, 2020, **8**, 14661–14670.
14 A. M. W. Dufter-Münster, A. G. Harter, T. M. Klapötke, E. Reinhardt, J. Römer and J. Stierstorfer, Lithium nitropyrazolates as potential red pyrotechnic colourants, *Eur. J. Inorg. Chem.*, 2022, **18**, e202101048.
15 T.-W. Wang, Z.-X. Yi, L. Zhang, Y.-K. Wang, Y. Li and J.-G. Zhang, Top development of green-light pyrotechnics: hypergolic Cu(II)-based coordination polymers, *Cryst. Growth Des.*, 2022, **23**, 558–564.
16 W. Cao, Y. Hu, T.-W. Wang, W.-S. Dong and J.-G. Zhang, Energetic metal salts of 3-(5-Amino-1,2,4-oxadiazol-3-yl)-1H-1,2,4triazol-5-nitramide: promising alternatives for environmentally friendly pyrotechnic components, *Cryst. Growth Des.*, 2023, **23**, 5621–5630.
17 H.-Y. Bian, Y.-F. Yan, M. Cui, T.-T. Song, X.-D. Guo, J.-G. Xu, F.-K. Zheng and G.-C. Guo, Energetic isostructural metal imidazolate frameworks with a bridging dicyanamide linker towards high-performance hypergolic fuels, *Inorg. Chem. Front.*, 2023, **10**, 5468–5474.
18 W.-Q. Zhang, X.-J. Qi, S. Huang, J.-S. Li and Q.-H. Zhang, Super-base-derived hypergolic ionic fuels with remarkably improved thermal stability, *J. Mater. Chem. A*, 2015, **3**, 20664–20672.

19 Z.-J. Lu, T.-W. Wang, M. Sun, M.-Q. Xu, C. Zhang, Z.-X. Yi and J.-G. Zhang, Synthesis of energetic coordination compounds based on pyrazole and 4-chloropyrazole via comelting crystallization method, *CrystEngComm*, 2024, **26**, 1178–1188.

20 R. B. Lv, J.-Y. Zhou, L. He, T.-W. Wang, H.-Z. Li and Q. Zhang, Azo-linked four-heterocyclic energetic molecule and its complexes: Exploring the important influence of conjugated planar structure on their crystal arrangement and stability, *Energ. Mater. Front.*, 2024, **5**, 17–26.

21 S.-L. Chen, Z.-R. Yang, B.-J. Wang, Y. Shang, C.-T. He, W.-X. Zhang and X.-M. Chen, Molecular perovskite high-energetic materials, *Sci. China Mater.*, 2018, **61**, 1123–1128.

22 S.-L. Chen, Y. Shang, C.-T. He, L.-Y. Sun, Z.-M. Ye, W.-X. Zhang and X.-M. Chen, Optimizing the oxygen balance by changing the A-site cations in molecular perovskite high-energetic materials, *CrystEngComm*, 2018, **20**, 7458–7463.

23 Y. Shang, R.-K. Huang, S.-L. Chen, C.-T. He, Z.-H. Yu, Z.-M. Ye, W.-X. Zhang and X.-M. Chen, Metal-free molecular perovskite high-energetic materials, *Cryst. Growth Des.*, 2020, **20**, 1891–1897.

24 W.-X. Zhang, S.-L. Chen, Y. Shang, Z.-H. Yu and X.-M. Chen, Molecular perovskites as a new platform for designing advanced multi-component energetic crystals, *Energ. Mater. Front.*, 2020, **1**, 123–135.

25 J. Wang, X.-X. Chen, L. Ye, Y.-P. Gong, Y. Shang and W.-X. Zhang, A room-temperature moisture-stabilized metal-free energetic ferroelectric material for piezoelectric generation, *Mater. Chem. Front.*, 2023, **7**, 2251–2259.

26 Y. Shang, S.-L. Chen, Z.-H. Yu, R.-K. Huang, C.-T. He, Z.-M. Ye, W.-X. Zhang and X.-M. Chen, Silver(I)-based molecular perovskite energetic compounds with exceptional thermal stability and energetic performance, *Inorg. Chem.*, 2022, **61**, 4143–4149.

27 Z.-H. Yu, D.-X. Liu, Y.-Y. Ling, X.-X. Chen, Y. Shang, S.-L. Chen, Z.-M. Ye, W.-X. Zhang and X.-M. Chen, Periodate-based molecular perovskites as promising energetic biocidal agents, *Sci. China Mater.*, 2023, **66**, 1641–1648.

28 S.-L. Chen, Y. Shang, J. Jiang, M. Huang, J.-T. Ren, T. Guo, C.-X. Yu, W.-X. Zhang and X.-M. Chen, A new nitrate-based energetic molecular perovskite as a modern edition of black powder, *Energ. Mater. Front.*, 2022, **3**, 122–127.

29 Y.-F. Huang, L. Xiang, Y. Feng, Z. An, L.-P. Miao, J.-R. Li, H.-Y. Ye and C. Shi, High quality of a perchlorate-based hybrid perovskite-type cage-like single crystal – evidence of temperature-induced distinct dielectric transition, *Eur. J. Inorg. Chem.*, 2021, 4439–4442.

30 J.-C. Zhou, B.-Y. Zhou, X.-J. Ma, T.-T. Cheng, N.-X. Li and H.-J. Xu, Synthesis, structure and properties of the first organic-templated inorganic-framework Ba(II) perchlorate, *J. Mol. Struct.*, 2011, **1006**, 441–446.

31 R. Meyer, J. Köhler and A. Homburg, *Explosives, 6th, Completely Revised Edition*, Wiley-VCH Verlag GmbH, 2007, pp. 337–339.

32 X. Biquard, O. Sublemontier, J. Berlande, M. A. Gaveau, J. M. Mestdagh and J. P. Visticot, Stabilization of barium dimers on clusters: reactions of Ba_2 with Cl_2 and O_2 on large argon clusters, *J. Chem. Phys.*, 1995, **103**, 957–965.

